Distribution of Grain Boundary Planes at Coincident Site Lattice Misorientations

Gregory S. Rohrer, Bassem S. El Dasher[1], Herbert M. Miller, Anthony D. Rollett, David M. Saylor[2]
Department of Materials Science and Engineering, Carnegie Mellon University,
Pittsburgh, PA 15213-3890, U.S.A.
[1]University of California, Lawrence Livermore National Laboratory, P.O. Box 808, Livermore, CA 94511, U.S.A.
[2]U.S.F.D.A., 12725 Twinbrook Parkway, Rockville, MD 20852, U.S.A.

ABSTRACT

The grain boundary plane distributions in MgO, $SrTiO_3$, $MgAl_2O_4$, and Al are compared at lattice misorientations with a coincident site density of greater than or equal to 1/9. In most situations, the most frequently adopted grain boundary orientation is a habit plane of low index and low surface energy that depends on the particular material. Cases where the most common boundary orientation is a plane of high planar coincident site density instead of a characteristic habit plane are rare. In fact, in most cases, the distributions of grain boundary planes at misorientations with high lattice coincidence are not substantially different from the distributions at other, more general misorientations. The results indicate that a model for grain boundary energy and structure based on grain surface relationships is more appropriate than the widely accepted models based on lattice orientation relationships.

INTRODUCTION

To distinguish one grain boundary from another, five independent parameters must be specified. If the parameters are measured with a resolution of Δ°, then as Δ decreases and the resolution increases, the number of distinguishable grain boundaries increases in proportion to $1/\Delta^5$. For example, in a cubic system, if the five angular parameters are measured with 10° of resolution, then there are approximately 6.5×10^3 distinct boundaries. By increasing the resolution to 5°, this number increases to 2×10^5. Historically, this complexity has been handled by assigning boundaries to broad categories, such as low misorientation angle grain boundaries, general boundaries, and coincident site lattice (CSL) boundaries. While reducing the number of grain boundary types to a manageable level, this approach obviously groups together many boundaries which are not identical in the crystallographic sense and may have very different properties. For example, when boundaries are classified by their coincident site lattice type, the two degrees of freedom that describe the interface plane remain unspecified. Because it has recently become possible to make comprehensive measurements of the grain boundary character distribution, it is now possible to classify boundaries by all five parameters. The purpose of this paper is to describe how the grain boundary planes are distributed at selected CSL misorientations in several polycrystalline materials.

The CSL concept has been in use for more than 50 years [1]. The basic idea is that boundaries with misorientations that place a high fraction of lattice sites in coincidence are distinguished from more general boundaries. These CSL boundaries are assigned a coincidence number (Σ) based on the inverse of the number of coincident lattice sites [2]. Therefore, a low Σ

number signifies high coincidence. After Aust and Rutter [3] reported that low Σ CSL boundaries in Sn-doped Pb migrated at a much higher rate than general boundaries, interest in these boundaries increased significantly. In the current era, the interest stems principally from the relevance of low Σ CSL boundaries to grain boundary engineering [4,5]. It has been reported that a range of macroscopic properties (for example, the resistance to corrosion) improve as the density of low Σ CSL boundaries increases.

It seems intuitive that boundaries between grains whose lattices exhibit partial coincidence would have lower energies and distinct properties. However, the lattice coincidence is likely to have physical significance only when it occurs in the boundary plane. Thus, while CSL boundaries are defined by misorientation, the condition of high coincidence is more restrictive; for a specific CSL misorientation, high coincidence at the interface occurs only at a few specific grain boundary plane orientations. To characterize the influence of the interface plane orientation on the coincidence within the boundary, the concept of the planar coincident site density (PCSD) was introduced [6,7]. This parameter characterizes the fraction of coincident sites within the boundary plane.

Measurements of the grain boundary plane orientation have not been widespread. This is largely because of the difficulty of doing this for a large number of boundaries. Of the possible ways of doing this, electron back scattered diffraction (EBSD) mapping coupled with serial sectioning is the most direct and readily available [8,9]. It should be recognized that the information in the EBSD map allows four of the five grain boundary parameters to be specified. This limits the possible planes to the zone of the grain boundary trace and using this condition, one can at least be certain about which grain boundary plane orientations are not possible. This principle has been used to determine how close the traces of Σ3 boundaries are to a zone containing the (111) plane [10,11]. More recently, a stereological procedure for quantitatively determining the distribution of grain boundary planes has been developed [12].

In the current paper, we define the grain boundary character distribution, $f(\Delta g, \mathbf{n})$, as the relative areas of grain boundaries distinguished by their lattice misorientation (Δg) and orientation ($\mathbf{n}$). By separating the three misorientation parameters and the two interface plane parameters, the distribution of grain boundary planes at each misorientation, $f(\mathbf{n}|\Delta g)$, can be plotted on a stereographic projection. Here, we consider in detail the Σ3, Σ5, Σ7, and Σ9 misorientations for four different cubic materials. The results are presented in multiples of a random distribution (MRD). Values greater than one indicate boundaries observed more frequently than expected in a random distribution. The resolution of the distribution is approximately 10 ° and the details of calculating this distribution are described in ref. 9.

EXPERIMENTAL DETAILS

The samples from which the data in this paper were derived, and the details of the data acquisition, have been described in prior publications [9, 13-16]. Pertinent aspects of each sample are described in Table I. In each case, crystal orientation maps of planar sections obtained by electron back scattered diffraction (EBSD) were the basis for the measurement of the grain boundary character distribution. In the case of MgO [9] and $SrTiO_3$ [13], data from parallel serial sections were used to determine the inclination of the grain boundary planes. For the cases of Al [16] and $MgAl_2O_4$ [14], the distribution was determined using a previously described stereological method [12]. The grain boundary character distribution, $f(\Delta g, \mathbf{n})$, is

parameterized and discretized as described in our previous work, and, therefore, has a resolution of approximately 10 °.

Table I. Materials Characteristics and Preparation

Material	Space group	Lattice parameter (Å)	Grain size (μm)	final heat, ° C, time, h	Source/preparation
MgO	$Fm\bar{3}m$	4.21	109	1600, 48 h	See reference 9
$SrTiO_3$	$Pm\bar{3}m$	3.90	90	1650, 48 h	See reference 13
$MgAl_2O_4$	$Fd\bar{3}m$	8.09	12	1600, 48 h	RCS Technologies, sintered disk.
Al	$Fm\bar{3}m$	4.05	30	400, 1 h	Alcoa, commercially pure alloy 1050

RESULTS

The distribution of grain boundary planes at the Σ3 misorientation, Σ(**n**||[111]/60°), in Al, $SrTiO_3$, and $MgAl_2O_4$, are shown in Fig. 1. Because of texture in the MgO specimen, the data for [111] misorientations are more difficult to interpret, so the distribution of planes at Σ3 and Σ7 are not presented. The pure twist configuration, bounded on both sides by (111) planes and also known as the coherent twin, occurs when the boundary normal (**n**) is parallel to the [111] misorientation axis. Pure tilt boundaries lie on a great circle 90 ° from the misorientation axis and these positions are shown on the stereogram by the great circle (dark line) in Fig. 1a. For all three materials, there is a clear maximum at the position of the coherent twin. The preference for this boundary configuration is strongest in Al and $MgAl_2O_4$, where the peaks are 28 and 6 MRD, respectively. It should be noted that all of the grain boundaries in these two materials tend to lie on planes with {111} orientations and (111) type twist boundaries are favored at all misorientations about the [111] axis [15, 16]. However, these Σ3 twist boundaries represent the maximum in the population for all [111] twist boundaries and, in fact, a global maximum at all points in the entire five parameter distributions of Al and $MgAl_2O_4$.

For $SrTiO_3$, there is also a maximum for the Σ3 coherent twin. However, it is relatively weak (1.7 MRD) and there are many other places in the distribution where the grain boundary population is higher. What is significant about this maximum is that it is contrary to the trend at all other misorientations in $SrTiO_3$, where {100} planes are favored and {111} planes are minima [13]. It is noteworthy that the (111)||[111]/60° boundary has a planar coincident site density of 2.31 sites/a^2, where a is the cubic lattice constant, and this is the highest PCSD of the interfaces discussed in this paper. For this lattice misorientation, the next highest density occurs for symmetric tilt boundaries with $(\bar{2}11)$, $(\bar{1}\,\bar{1}2)$, and $(1\bar{2}1)$ orientations, where the planar coincident site density is 0.82 sites/a^2. Note that these symmetric tilt boundaries are consistently local minima in the distribution.

The distributions of grain boundary planes at the Σ5 misorientation, Σ(**n**||[100]/37°), in Al, MgO, $SrTiO_3$, and $MgAl_2O_4$, are shown in Fig. 2. In this situation, the misorientation axis lies in the plane of the paper. In all four cases, the maxima in the populations are relatively low. There is a very similar structure for MgO and $SrTiO_3$: maxima occur at twist configurations comprised of two {100} planes and at asymmetric tilt boundaries made up of {001} and {034} planes. In Al and $MgAl_2O_4$, the maxima are found along small circles of boundaries with mixed tilt-twist

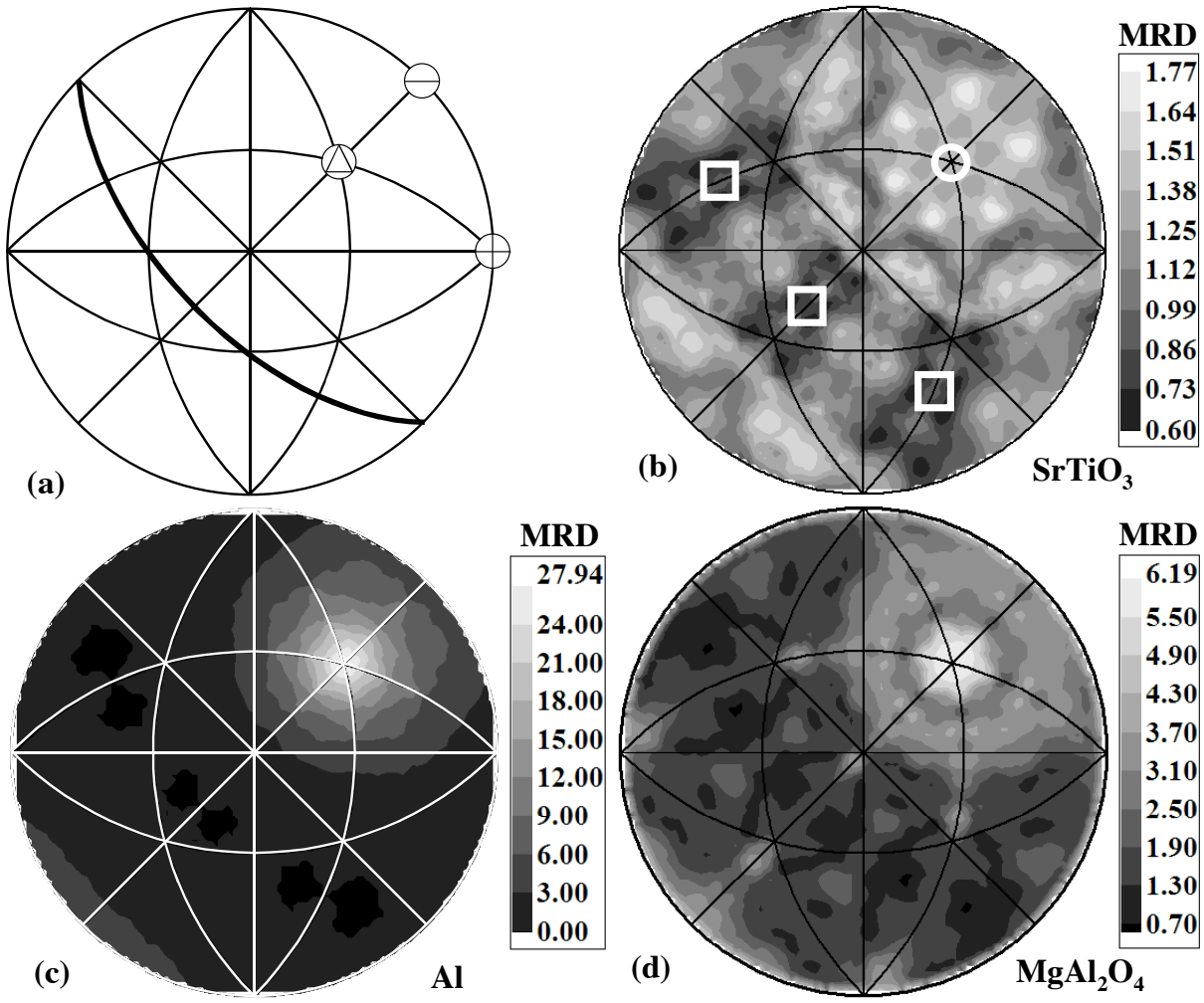

Figure 1. Observed grain boundary plane distributions for the Σ3 grain boundary, Σ(**n**|60°/[111]). (a) Schematic of the reference frame for the [001] stereographic projections. The [111] misorientation axis is marked by the circled triangle and shows the position of twist boundaries. The positions of the tilt boundaries are shown by the dark line and the [100] and [110] directions are denoted by the circled + and -, respectively. (b) $SrTiO_3$ (c) Al, and (d) $MgAl_2O_4$. In (b), the squares mark the position of the symmetric tilts and the circles the positions of the pure twist boundary. Twist: (111), tilt: $(\bar{2}11)$, $(\bar{1}\,\bar{1}2)$, and $(1\bar{2}1)$.

character that go through the (110) and (111) orientation. The orientations of high planar coincident site density (twist: (100) and $(\bar{1}00)$ tilt: (031), (012), $(0\,\bar{1}3)$, and $(0\bar{2}1)$) are marked on Fig. 2b. The (100) twist boundary has a planar coincident site density of 0.4 sites/a^2, the value at that symmetric {210} tilt is 0.89 sites/a^2, and the symmetric {310} tilt has a PCSD of 0.63 sites/a^2. Note that the orientations of the symmetric tilt boundaries occur at minima in the distributions for MgO and $SrTiO_3$. In the case of Al, there is a local maximum at the {012} tilt boundary, but the value is still smaller than expected in a random distribution. While the twist configuration of (001) planes is a maximum in MgO and $SrTiO_3$, this peak occurs for all [100] twist boundaries, regardless of the misorientation angle [9]. In other words, while there is a peak

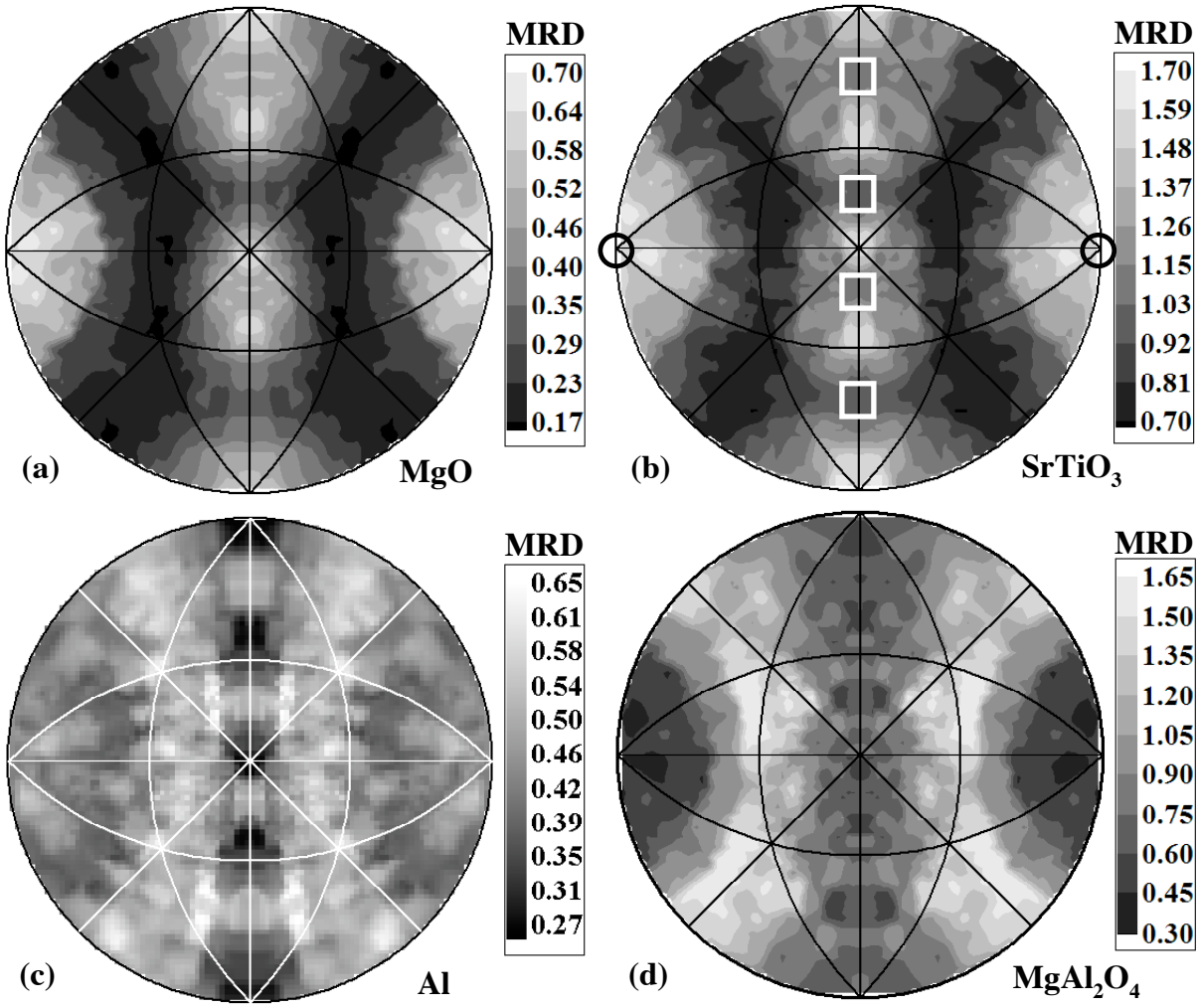

Figure 2. Observed grain boundary plane distributions for the Σ5 grain boundary, Σ(**n**|[100]/37°). The reference frame for the projection is the same as in Fig. 1, but now the misorientation axis lies in the plane of the page and is parallel to the [100] direction. (a) MgO, (b) $SrTiO_3$ (c) Al, and (d) $MgAl_2O_4$. In (b), the squares mark the position of the symmetric tilts and the circles the positions of the pure twist boundaries. Twist: (100) and $(\bar{1}00)$ tilt: (031), (012), $(0\,\bar{1}3)$, and $(0\bar{2}1)$.

for the (100)|[100]/37° boundary, the population is the same for other twist configurations where the planar coincident site density is zero. Therefore, this feature in the population is best explained by the occurrence of the favored {100} planes on either side of the interface.

At the Σ7 lattice misorientation, Σ(**n**|[111]/38°), Al shows a well defined peak for planes whose normals are parallel to the misorientation axis (see Fig. 3). As in the case of the Σ3, this is the pure twist configuration that places two (111) planes in opposition. A similar maximum is observed for spinel, but in this case, there are additional peaks at the other planes in the {111} family. The geometrically required complements to these boundaries have orientations rotated by 38° about [111] and this produces the pairs of maxima. The grain boundary plane distribution

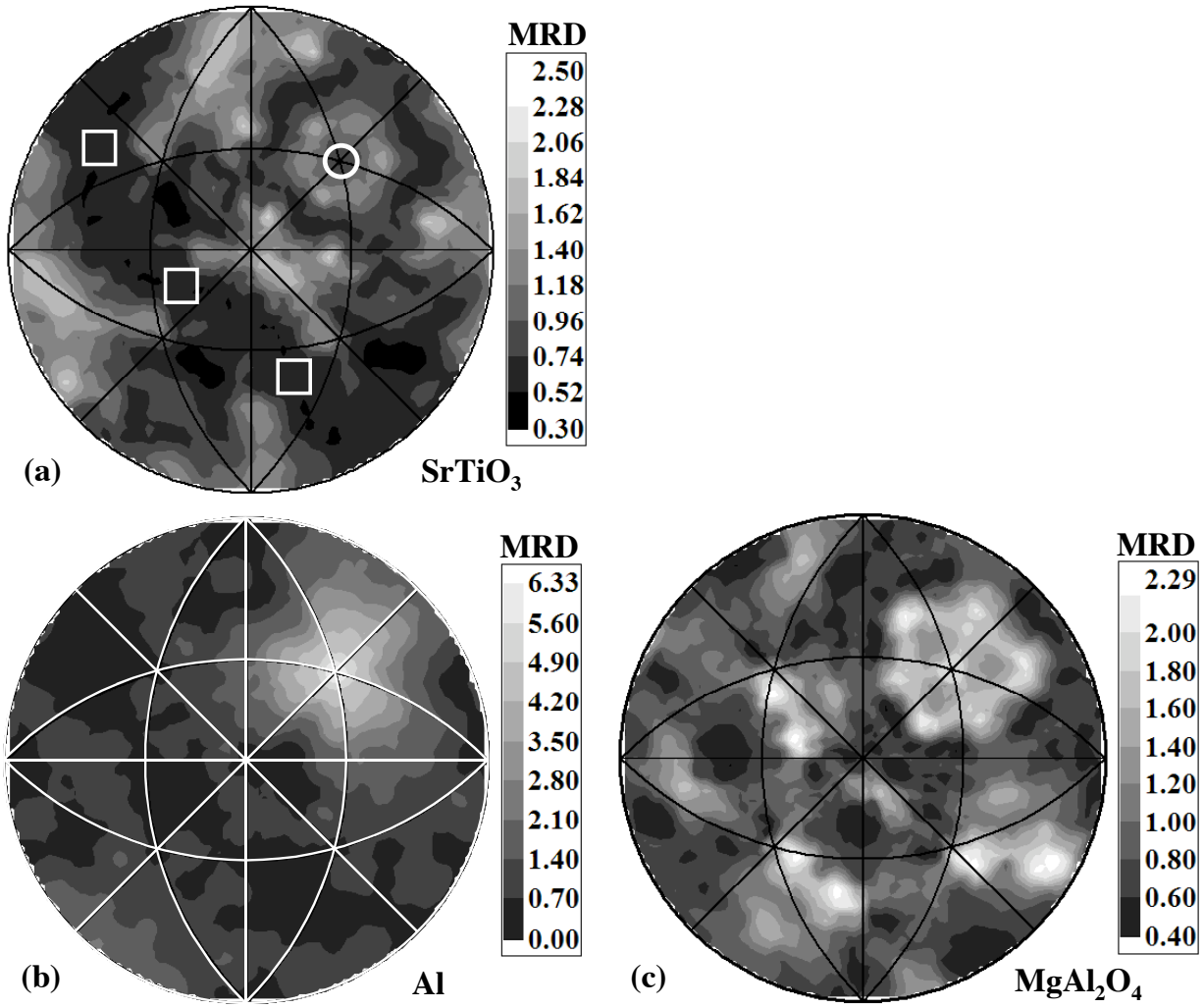

Figure 3. Observed grain boundary plane distributions for the Σ7 grain boundary, Σ(**n**|38°/[111]). The reference frame for the projection is the same as in Fig. 1. (a) $SrTiO_3$ (b) Al, and (c) $MgAl_2O_4$. In (a), the squares mark the position of the symmetric tilts and the circles the positions of the pure twist boundaries. Twist: (111), tilt: $(\bar{3}21)$, $(\bar{2}\bar{1}3)$ and $(1\bar{3}2)$.

for $SrTiO_3$ also exhibits a local maximum at the {111} twist position, but planes oriented near {100}-type orientations have a higher intensity. So, all of the boundary plane distributions show some preference for the pure twist configuration, which has a planar coincident site density of 0.33 sites/a^2. However, in the case of Al and $MgAl_2O_4$, this configuration matches the preferred (111) habit planes and this situation is favored at all misorientations. The other planes with a high planar coincident site density are the symmetric tilts: $(\bar{3}21)$, $(\bar{2}\bar{1}3)$ and $(1\bar{3}2)$, which have a density of 0.18sites/a^2. Note that the distributions all reach a minimum at these orientations.

At the Σ9 lattice misorientation, Σ(**n**|39°/[110]), planes of maximum planar coincidence occur for the pure twist configuration, on (110) and $(\bar{1}\,\bar{1}0)$, where the PCSD is 0.16 sites/a^2, and the tilt configuration, on $(\bar{2}21)$ and $(1\,\bar{1}4)$, where the PCSD is 0.67 and 0.47 sites/a^2, respectively. The distributions of grain boundary planes at this misorientation are shown in Fig. 4 and the planes of high PCSD are marked on Fig. 4a. In each case, the twist configuration has a

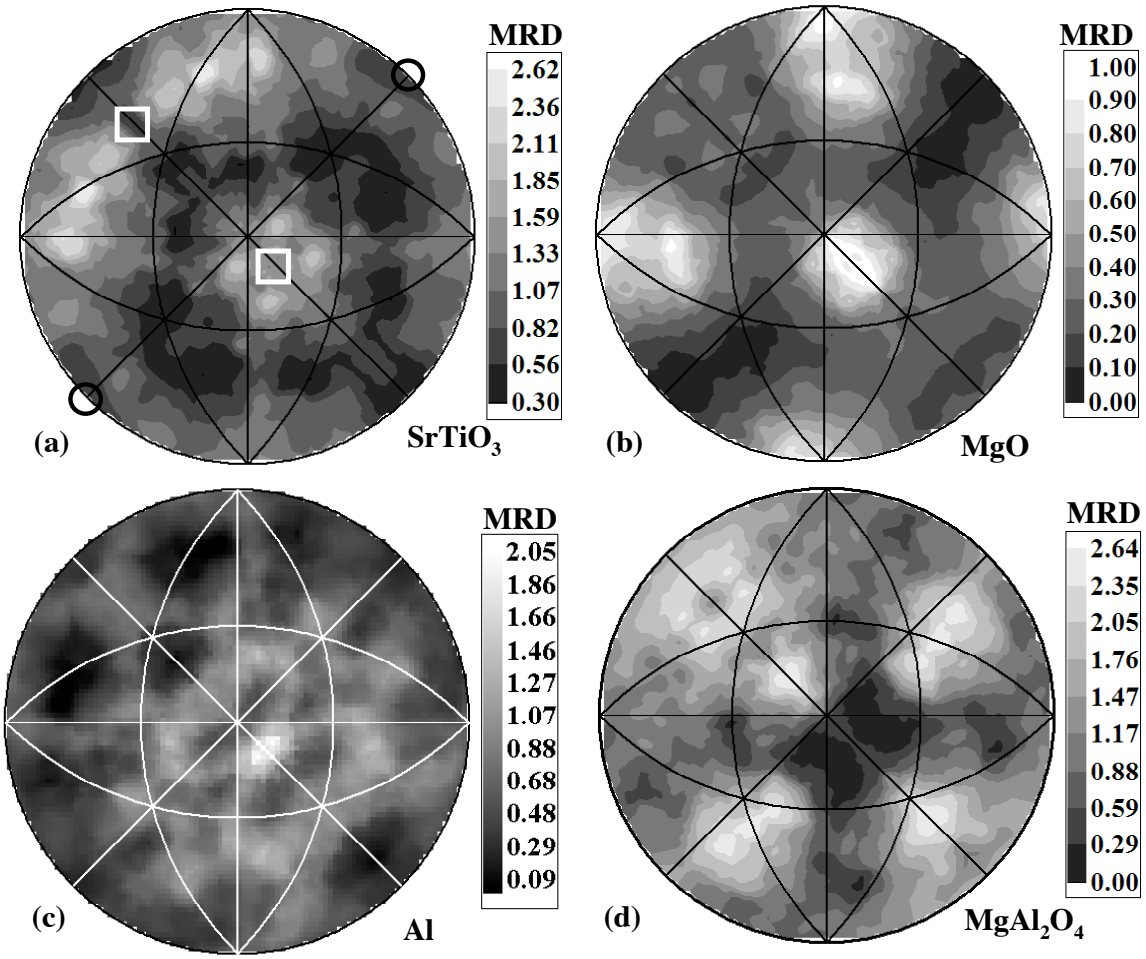

Figure 4. Observed grain boundary plane distributions for the Σ9 grain boundary, Σ(**n**|39°/[110]). The reference frame for the projection is the same as in Fig. 1, but now the misorientation axis lies in the plane of the page and is parallel to the [110] direction. (a) $SrTiO_3$, (b) MgO, (c) Al, and (d) $MgAl_2O_4$. In (a), the squares mark the position of the symmetric tilts and the circles the positions of the pure twist boundaries. Twist: (110) and $(\bar{1}\,\bar{1}0)$, tilt $(\bar{2}21)$ and $(1\,\bar{1}4)$.

low population. The distribution of grain boundary planes in Al shows a maximum at the $(1\,\bar{1}4)$ symmetric tilt boundary. There is also a local maximum near this position in the distribution of planes in MgO and $SrTiO_3$, but when compared to the distributions at other misorientation angles, the elevated population results from the proximity of the dominant (001) and the asymmetric plane in the zone of tilts inclined by 39° from (001) which overlap at the $(1\,\bar{1}4)$ orientation [9]. This is consistent with the appearance of maxima at other {100} type positions in the distribution shown in Fig. 4a and 4b. The distribution of planes in $MgAl_2O_4$ shows only local minima at the positions of high planar coincidence.

DISCUSSION

In the interpretation of the data presented in this paper, it should be noted that because misorientation space has been discretized in approximately 10° increments, the distribution of grain boundary planes at each CSL misorientation are averaged with those of neighboring misorientations within a 10° window. Thus, if there are cusps in the distribution at the CSL misorientations, the true population will be diluted by the coarse discretization. The effect is that extreme values move closer to the average. Thus, while the discretization may cause us to underestimate the actual values at the extreme positions in the distribution, it doesn't alter the basic observation that in most cases, it is the interface that combines preferred habit planes that is favored, not necessarily the interface with the maximum planar coincidence.

Based on prior work, it has become apparent that there is a connection between the grain boundary population, $P(\Sigma g, \mathbf{n})$, and the grain boundary energy [17, 18]. It has long been assumed that there is an inverse correlation between the two quantities. In the case of MgO, the relative grain boundary energy, $\gamma(\Sigma g, \mathbf{n})$, has been determined by analyzing the dihedral angles of triple junctions and it was found that there is a strong correlation between the grain boundary energy and the population [17]. Boundaries with high relative energy are observed less frequently than boundaries with a low relative energy, and a similar observation was reported for Al [18]. Throughout this discussion, it will be assumed that the inverse correlation between grain boundary energy and grain boundary population also holds in $SrTiO_3$ and $MgAl_2O_4$.

In aggregate, the data presented here suggest that the occurrence of low energy and high population grain boundary orientations are more consistent with an explanation based on the grain surface orientation than one based on planar coincidence in the interface plane. This can be summed up with the statement that grain boundary planes in bicrystals with a lattice coincidence of greater than or equal to 1/9 are more likely to take the orientation of a low index plane characteristic of the particular material than they are to take an orientation with an especially high geometric planar coincidence. In fact, the trends in the plane distributions at the low sigma CSL misorientations are the same as those found at general misorientations. The main exceptions to this trend occur at the $\Sigma 3$ misorientation in $SrTiO_3$ and the $\Sigma 9$ misorientation in Al.

The $\Sigma 3$ pure twist configuration, which consists of two parallel (111) planes, is always a maximum in the distribution. While this is not surprising for Al and $MgAl_2O_4$, which both prefer (111) habit planes at all misorientations, it is not expected for $SrTiO_3$. At all other misorientations, $SrTiO_3$ grain boundaries are made up of {100} planes and their geometrically necessary complements [13]. It should be noted that in comparison to the other boundaries described here, the planar coincident site density at the $\Sigma 3$ twist is more than twice that of any other interface. We assume that because of this extraordinary planar coincidence, it has a much lower energy than in other boundaries and this is responsible for its relatively high population.

Support for the idea that the $\Sigma 3$ pure twist boundary has a low energy can be found in many sources: experiments on Al [18], NiO [19], MgO [20], and a Ni-Cr-Fe [21] alloy all indicate that this boundary has a relatively low energy, and this observation is consistent with the results of simulations [22]. Further, the experiments on [110] symmetric tilt bicrystals demonstrate that the $\Sigma 3$ misorientation alone is not a sufficient condition for low energy. Rotations of 70.53° and 109.47° about [110] are both $\Sigma 3$ misorientations; however, a high degree of coincidence in the intergranular region occurs only for symmetric {111} boundary planes. This configuration is realized by a symmetric 70.53° rotation, but not for the symmetric 109.47° rotation. In the case

of MgO, the energy of 109.47° Σ3 rotation was approximately 40% higher than the 70.53° Σ3 rotation [20]. The effect was even larger in the NiO case where the energy of the 109.47° Σ3 rotation was 300% higher than the 70.53° Σ3 rotation [19].

Previous data on Σ5 boundaries of high planar coincidence have contradictory results. Studies of symmetric [100] boundaries in Cu [23], Al [18], and NiO [24, 25] show no sign of a cusp in the grain boundary energy as a function of misorientation. Computer simulations of (100) twist boundaries do not reveal a singularity at the Σ5 misorientation and only very modest cusps for the symmetric (210) and (310) tilt boundaries [22]. On the other hand, symmetric (100) twist grain boundaries in Si showed a narrow and shallow cusp at the Σ5 misorientation [26] and a study of symmetric (100) twist grain boundaries in MgO indicate the presence of a cusp at the Σ5 misorientation [20], but this is inconsistent with more recent studies [27]. In the materials examined here, there is no evidence that Σ5 boundaries with high PCSD have energies that are lower than other configurations comprised of low index habit planes.

Grain boundaries with the Σ7 lattice misorientation clearly favor low index habit planes. In the case of Al and $MgAl_2O_4$, these are (111) planes and this leads to a high density of twist boundaries. However, for $SrTiO_3$, (100) habit planes are preferred. Tilt boundaries of high planar coincident site density are not favored in any of these three materials.

Measurements of the energy of symmetric Σ9 tilt boundaries frequently indicated that these boundaries have a reduced energy, although it is usually a modest reduction. For example, in Al [18], MgO [20], and NiO [19], the Σ9 boundary on the (221) plane was observed to have a reduced energy. Measurements of the energy of Σ9 grain boundaries of indeterminate orientation in MgO [28] indicated that their energy was at or above the average while similar measurements in a Ni-Cr-Fe alloy [21] indicated that they do have a reduced energy. The present data show no indication that the population of this boundary is greater than that of other boundaries at the same lattice misorientation. Instead, in MgO, $SrTiO_3$, and $MgAl_2O_4$, we find a preference for the same habit planes that occur at other misorientations. In Al, on the other hand, the symmetric {114} boundary is favored. It is not clear why this configuration is selected over the symmetric {221} boundary, which has a higher PCSD.

That the energies and populations of grain boundaries correspond to low index, low energy planes can be understood in terms of the surface energy anisotropy. If we imagine creating a grain boundary by first creating the two free surfaces and then joining them, we can say that the boundary energy is the sum of the two surface energies, minus a binding energy that results from the interactions of the atoms on either side of the interface [22]. The observed correlation between the grain boundary and surface energies indicates that this binding energy is approximately constant for different boundaries, or that it increases as the average energy of the surfaces adjoining the boundary decreases. We assume that because of the remarkable planar coincidence of the Σ3 (111) twist configuration, this boundary is favored in $SrTiO_3$ over those consisting of {100} planes. In the case of the symmetric Σ9 {114} boundary in Al, it is not clear why this plane is selected over others with a lower surface energy or a higher planar coincident site density. However, we note that the surface energy anisotropy and the grain boundary plane anisotropy are both very low in Al and in this case, the local structure of the boundary plane might have a decisive influence by increasing the binding energy by more than enough to account for the modest increase in the energy of the surfaces adjoining the grain boundary.

CONCLUSIONS

The distribution of grain boundary planes in bicrystals with a lattice coincidence of greater than or equal to 1/9 are more likely to take the orientation of a low index plane characteristic of the particular material than they are to take an orientation with an especially high geometric planar coincidence. The main exceptions to this trend occur at the $\Sigma 3$ misorientation in $SrTiO_3$ and the $\Sigma 9$ misorienation in Al. The results indicate that a model for grain boundary energy and structure based on grain surface relationships is more appropriate than the widely accepted models based on lattice orientation relationships

ACKNOWLEDGEMENTS

This work was supported primarily by the MRSEC program of the National Science Foundation under award number DMR-0079996.

REFERENCES

[1] M.L. Kronberg and F.H. Wilson, Met. Trans. **185**, 501 (1949).
[2] H. Grimmer, W. Bollmann, and D.H. Warrington, Acta Cryst. **A30**, 197 (1974).
[3] K.T. Aust and J.W. Rutter, Trans. TMS-AIME **215**, 119 (1959).
[4] V. Randle, The role of the Coincident Site Lattice in Grain Boundary Engineering, Institute of Materials, London, 1996.
[5] G. Palumbo, E.M. Lehockey, and P. Lin, JOM Feb., 40 (1998).
[6] D.G. Brandon, B. Ralph, S. Ranganathan, and M.S. Wald, Acta Metall. **12**, 813 (1964).
[7] B. Chalmers and H. Gleiter, Phil. Mag. **23**, 1541 (1971).
[8] V. Randle and H. Davies, Ultramicroscopy **90**, 153 (2002)
[9] D.M. Saylor, A. Morawiec, and G.S. Rohrer, Acta Mater. **51** 3663 (2003).
[10] H. Davies and V. Randle, J. Microscopy **205**, 253 (2002).
[11] Wright, J. Bingert, T.A. Mason, and R.J. Larsen, Mater. Sci. Forum **408-12**, 511 (2002).
[12] D.M. Saylor, B.L. Adams, B.S. El Dasher, G.S. Rohrer, Met. Mater. Trans., in press.
[13] D.M. Saylor, B.S. El-Dasher, T. Sano, G.S. Rohrer, J. Amer. Ceram. Soc. **87**, 670 (2004).
[14] D.M. Saylor, B.S. El-Dasher, Y. Pang, H.M. Miller, P. Wynblatt, A.D. Rollett, G.S. Rohrer, J. Amer. Ceram. Soc. **87**, 724 (2004).
[15] H.M. Miller, D.M. Saylor, B.S. El Dasher, A.D. Rollett, G.S. Rohrer, Crystallographic Distribution of Internal Interfaces in Spinel Polycrystals. In: Second International Conference on Recrystallization and Grain Growth, submitted.
[16] D.M. Saylor, B.S. El-Dasher, A.D. Rollett, G.S. Rohrer, Acta Mater., in press.
[17] D.M. Saylor, A. Morawiec, G.S. Rohrer, J. Amer. Ceram. Soc. **85**, 3081(2002).
[18] G.C. Hasson and C. Goux, Scripta Metall. **5**, 889 (1971).
[19] G. Dhalenne, M. Dechamps, and A. Revcolevschi, J. Amer. Ceram. Soc. **65**, C11 (1982).
[20] S. Kimura, E. Yasuda, and M. Sakaki, Yogyo-Kyokai-Shi **94**, 795 (1986).
[21] T. Skidmore, R.G. Buchheit, and M.C. Juhas, Scripta Mater. **50**, 873 (2004).
[22] D. Wolf, J. Mater. Res., **5**, 1708 (1990).
[23] N.A. Gjostein and F.N. Rhines, Acta Metall. **7**, 319 (1959).
[24] D.W. Readey and R.E. Jech, J. Amer. Ceram. Soc., **51**, 201 (1968).
[25] G. Dhalenne, A. Revcolevschi, and A Gervais, Phys. Stat. Sol (a) **56**, 267 (1979).

[26] A. Otsuki, Acta Mater. **49**, 1737 (2001).
[27] D.M. Saylor, A. Morawiec, and G.S. Rohrer, Acta Mater. **51**, 3675 (2003).
[28] D.M. Saylor, A. Morawiec, B.L. Adams, and G.S. Rohrer, Interface Science **8**, 131 (2000).